



## African Journal of Biological Sciences



Research Paper

Open Access

### Role of Dynamic Magnetic Resonance Imaging in characterization of benign and malignant Breast mass lesions

Marwa Mohammed salama, Fathy Ahmed Tantawy, Ahmed Sabry Ragheb, Mohammed Ibrahim Amin

Department of Radiodiagnosis, Faculty of Medicine, Zagazig University, Egypt

Email: [marwasalama774@gmail.com](mailto:marwasalama774@gmail.com)

#### Article History

Volume 6, Issue 2, April 2024

Received: 3 June 2024

Accepted: 11 July 2024

Published: 11 July 2024

doi:

10.48047/AFJBS.6.2.2024.1633-1652

**Abstract: Background:** Magnetic resonance imaging (MRI) of the breast is being performed more frequently to improve primary and recurrent tumor detection, characterization, and response to therapy. Sensitivity of this test approaches 90% and the specificity ranges from 37% to 100%. Magnetic resonance imaging (MRI) is a well-established method in breast imaging, with manifold clinical applications, including the non-invasive differentiation between benign and malignant breast lesions, preoperative staging, detection of scar versus recurrence, implant assessment, and the evaluation of high-risk patients. At present, dynamic contrast-enhanced MRI is the most sensitive imaging technique for breast cancer diagnosis, and provides excellent morphological and to some extent also functional information. To compensate for the limited functional information, and to increase the specificity of MRI while preserving its sensitivity, additional functional parameters such as diffusion-weighted imaging and apparent diffusion coefficient mapping, and MR spectroscopic imaging have been investigated and implemented into the clinical routine. Several additional MRI parameters to capture breast cancer biology are still under investigation. MRI at high and ultra-high field strength and advances in hard- and software may also further improve this imaging technique.

**Keywords:** *Magnetic resonance imaging, breast mass*

#### Introduction

Magnetic resonance imaging (MRI) is an essential tool in breast imaging with multiple clinical indications, including preoperative staging, monitoring of neoadjuvant chemotherapy, differentiation between scar and recurrence, evaluation of breast implants, evaluation of patients with cancer of unknown primary (CUP), and screening of high-risk patients (1, 2). When lesions are found to be suspicious on mammography, digital breast tomosynthesis, or sonography, MRI provides further non-invasive analysis and can obviate unnecessary biopsies (3). When breast cancer is detected or confirmed, MRI provides concurrent staging of disease for treatment planning. Dynamic contrast-enhanced MRI (DCE-MRI) offers morphological and functional tumour information, with excellent sensitivity and variable specificity for breast cancer diagnosis

(4–6). To overcome limitations in specificity and assess more functional data, additional MRI parameters can be combined with DCE-MRI; this approach is defined as multiparametric MRI (MP MRI) and has been successfully implemented in clinical routine. Recent studies demonstrated that MP MRI can provide additional information regarding the hallmarks of cancer, thereby increasing its specificity (7–9). Diffusion-weighted imaging (DWI) and proton MR spectroscopy imaging (<sup>1</sup>H-MRSI) are examples of techniques that are already established in breast imaging for providing additional parameters, while newer techniques such as chemical exchange saturation transfer (CEST), blood oxygen level-dependent (BOLD), sodium imaging (<sup>23</sup>Na-MRI), phosphorus spectroscopy (<sup>31</sup>P-MRSI), lipid MRSI or hyperpolarised MRI (HP MRI) are still being investigated. Meanwhile, breast MRI is steadily moving to 3 T and even 7 T, as the application of high and ultra-high field strengths can improve diagnostic accuracy of breast cancer detection. Abbreviated MRI protocols for breast cancer assessment and screening are currently being developed.

#### DYNAMIC CONTRAST-ENHANCED MRI (DCE-MRI)

DCE-MRI is the backbone of any MRI protocol, enabling the simultaneous assessment of tumour morphology and semi-quantitative enhancement kinetics that evaluate neoangiogenesis as a tumour-specific feature (4, 7). Cancers typically develop abnormal vasculature and increased vessel permeability to support its high metabolic demand for oxygen and nutrients (10). At present, DCE-MRI is generally recognised as the most sensitive imaging modality and aids in the non-invasive differentiation of benign and malignant lesions, while it may obviate unnecessary breast biopsies (6, 11, 12).

In 2003, the American College of Radiology (ACR) introduced the Breast Imaging-Reporting and Data System (BI-RADS) MRI lexicon to standardize breast MRI reports worldwide; a revised version was released in 2013 (13). This lexicon provides a standardized terminology for breast MRI findings, report structure, and classification system. The final BI-RADS category determines the probability of malignancy and is based on the most suspicious finding in each breast. A BI-RADS category 0 is assigned when the examination is incomplete, while category 1 indicates a negative examination, category 2 a benign, and category 3 a probably benign lesion. A BI-RADS category 4 suggests that the finding is suspicious enough to justify biopsy, while category 5 is highly suggestive of malignancy, and category 6 is assigned in the case of a histologically verified malignancy.

#### Imaging parameters

Image acquisition is performed in an axial plane with 2 mm (or finer) sections. Sagittal and coronal reconstructions are made from this dataset. Sagittal image acquisition is usually preferred for biopsy procedures. The primary pulse sequences are fat-suppressed axial T1-weighted (T1W) without and with contrast and fat suppressed axial T2-weighted (T2W) or short TI inversion recovery (STIR). For the contrast portion of the exam, a paramagnetic gadolinium-based intravascular contrast (0.1 mmol/kg) is injected at a rate of 2 mL/s. A minimum of two postcontrast T1-weighted series should be obtained, with initial post-contrast images within 2 minutes and delayed post-contrast images within 8 min after contrast administration. Kinetic curves are generated from these T1W post-contrast images. Fat suppression is used because an enhancing cancer can be confused with nonsuppressed fat as they both have high signal intensity on T1W images. The most common way to reduce or remove fat signal and show enhancement more clearly is to use spectral fat saturation. Homogeneous fat suppression may not be possible with large breasts.

#### Image interpretation

##### ACR BI-RADS® Lexicon

The American College of Radiology (ACR) has created a breast imaging and reporting data system (BI-RADS®) atlas [2,3] which contains terminology for describing lesion architecture and enhancement characteristics. Use of this terminology allows a comprehensive analysis of both morphological and kinetic features used in image interpretation and helps radiologists and other clinicians communicate more clearly and consistently. A radiological description should include lesion information including clock-face location and distance from nipple, morphologic assessment of enhancement, associated findings such as nipple retraction or inversion and skin changes (retraction, thickening, and invasion), and a kinetic curve assessment [Table 1].

Category	Classification
Background enhancement of breasts	Minimal, mild, moderate, marked
Lesion location	Clock-face; distance from nipple
Enhancement type	Focus: < 5 mm Mass: 3 dimensional lesion
Mass characteristics	Shape: Round, oval, lobulated, irregular Margins: Smooth, irregular, spiculated
Morphologic assessment of enhancement	Mass or non mass like
Internal enhancement of mass or non mass like enhancement	Homogenous, heterogeneous, rim, dark internal septations, enhancing internal septations, and central Distribution: Focal, linear, ductal, segmental, regional, diffuse Internal enhancement: Homogenous, heterogeneous, clumped, stippled or punctate, reticular or dendritic
Enhancement kinetics	Symmetric or asymmetric Type I, II, or III curve
Diffusion-weighted imaging	Restricts diffusion; does not restrict diffusion
Associated findings	Nipple retraction; skin changes (retraction, thickening, invasion)

### Background enhancement

Assessment of background parenchymal enhancement pattern can be described with 4 M's: minimal, mild, moderate, and marked. This is analogous to mammographic breast tissue density in that breasts with greater background enhancement (or greater density in mammography) may limit accuracy of underlying lesion detection.[4] Background parenchymal enhancement fluctuates with the menstrual cycle, being highest during weeks 1 and 4 and lowest during week 2. Thus, imaging between days 7–14 of the menstrual cycle is recommended, unless precluded by clinical urgency. With background enhancement in mind, one must determine if there is a lesion that is conspicuous among its surroundings.

### Morphologic assessment of enhancement

A lesion of less than 5 mm should be described as a focus. A focus or multiple foci may result from hormonal changes (eg, fibrocystic changes) and are often stable on follow-up exams.

A 3-dimensional lesion (mass) should be characterized according to shape (round, oval, lobulated, or irregular), margins (smooth, irregular, or spiculated), and internal enhancement (homogenous, heterogeneous, rim, dark internal septations, enhancing internal septations, or central). More irregular and spiculated masses have a higher likelihood of malignancy. Specific internal enhancement patterns are often associated with certain entities: rim-enhancement is seen with high-grade invasive ductal carcinoma, cysts with inflammation, and fat necrosis; dark internal septations may be seen with fibroadenomas; enhancing internal septations are often seen with malignancy; central enhancement is seen with high-grade ductal carcinoma and vascular tumors.

If enhancement is located in an area that is not associated with a mass (nonmasslike enhancement), the description should give details of the distribution (focal, linear, ductal, segmental, regional, or diffuse), internal enhancement (homogenous, heterogeneous, clumped, stippled, punctate, reticular or dendritic), and whether it is symmetric or asymmetric. Ductal and segmental distribution of enhancement can be seen with ductal carcinoma *in situ* (DCIS) or invasive ductal cancer, sclerosing adenosis, atypical ductal hyperplasia, or papillary neoplasms. Diffuse enhancement is seen with benign processes and normal fibroglandular tissues. Reticular or dendritic internal enhancement is seen with lymphatic involvement such as that seen with inflammatory breast cancer.

### Enhancement kinetics

Three basic curve shapes have been described [Figure 1].[5] Type-I curves are slowly enhancing, in which gradual, steady enhancement occurs over about 5 min. Malignancy is seen in approximately 6% of lesions

with a Type-I curve.[6] Type-II curves show early strong enhancement (increase over a 1–2 min period) with a subsequent plateau phase. Malignancy is seen in approximately 6–29% of lesions with a Type-II curve.[6] Type III or “washout” curves show early strong enhancement (over 1–2 min), with subsequent decline in enhancement. This produces a characteristic peak dubbed the “the cancer corner,” and is strongly associated with malignancy. Malignancy is seen in approximately 29-77% of lesions with a Type-III curve.[6] Both Type-II and Type-III curves should be considered suggestive of malignancy.

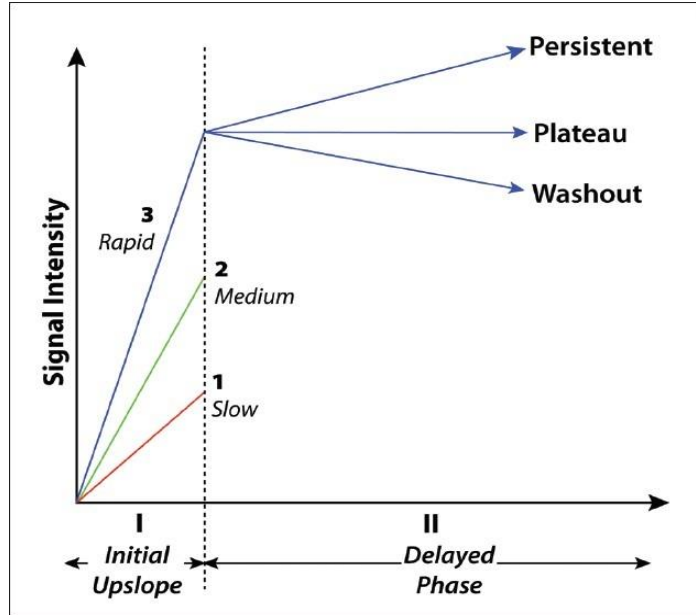


**Figure 1**

Three types of enhancement kinetics curves seen with breast MRI.

Diffusion-weighted imaging (DWI) is a technique that takes into account the differences in diffusion rate of water molecules in normal and pathologic tissue. This technique, although not commonly used, has a higher specificity to differentiate between benign and malignant breast lesions compared to that of contrast-enhanced MRI (84% compared to 37%).[7] It relies on differences in cellularity to distinguish between benign and malignant lesions. Malignant lesions, which frequently have a higher degree of cellularity compared with benign lesions, often demonstrate restricted diffusion.

**Computer-aided detection in breast MRI**

Computer-aided detection (CAD) can be performed using a software adjunct package for enhancement kinetics. A maximal intensity projection (MIP), kinetics curve, and color map overlay can be generated [Figure 2]. CAD does not evaluate anatomy or pathology. Advantages of CAD include the ability to quickly analyze large numbers of images, aid in visual subtraction, and facilitate reconstructions and future comparisons.

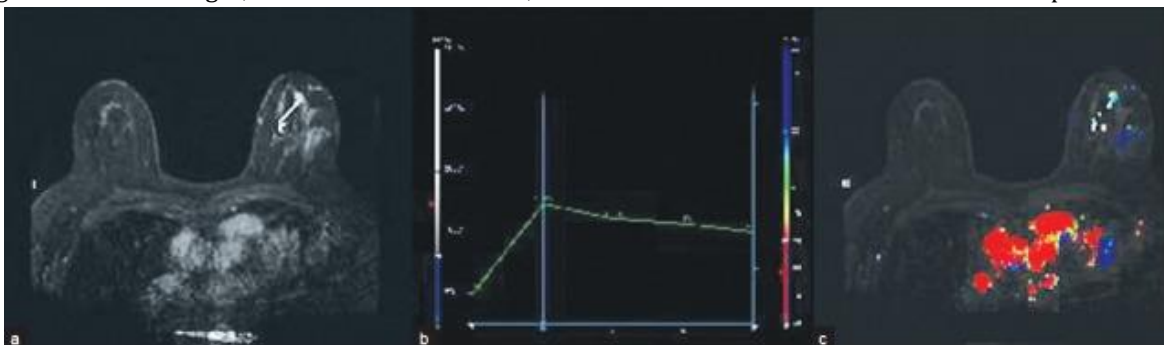


**Figure 2**

(a) MIP, (b) kinetics curve, and (c) color map overlay obtained using CAD software.

### Artifacts

Breast MRI is susceptible to artifacts common in MRI of all organ systems: ghosting, motion, wrap-around, magnetic susceptibility, signal void, field inhomogeneity, and chemical shift. Artifacts specific to breast imaging include background parenchymal enhancement (discussed above), which can be avoided by imaging between days 7–14 of the menstrual cycle, and artifact due to breast tissue (usually large breasts) abutting the radiofrequency coil, leading to signal voids and magnetic susceptibility. Poor fat saturation, which can be due to incorrect identification of the fat peak or field inhomogeneity, is often seen with breasts composed of larger amounts of fat. Care must be taken that the proper fat peak is selected, shimming is used to improve field uniformity, and appropriately sized breast coils are used to ensure adequate fat suppression.

### Common benign lesions

Benign breast lesions can have a variable appearance on MRI. However, a few important principles regarding benign lesions have been described. Lesions with high signal on T1W imaging often contain fat and are thus most often benign, unless they are rapidly growing. Lesions that show intensely high signal on T2W imaging often contain water and are also generally benign. One important exception is colloid carcinoma, which also exhibits high signal on T2W images. Benign lesions often do not show enhancement. However, as described above, variable enhancement kinetics can be seen with benign lesions. Benign lesions often do not show restricted diffusion.

A *simple cyst* is the most common benign breast lesion. It is best seen with ultrasound as a well circumscribed, anechoic mass, with an imperceptible wall and posterior acoustic enhancement. On MRI, simple cysts show low signal on T1W images, high signal on T2W images, and do not enhance. Mammography cannot distinguish between cyst and solid mass.

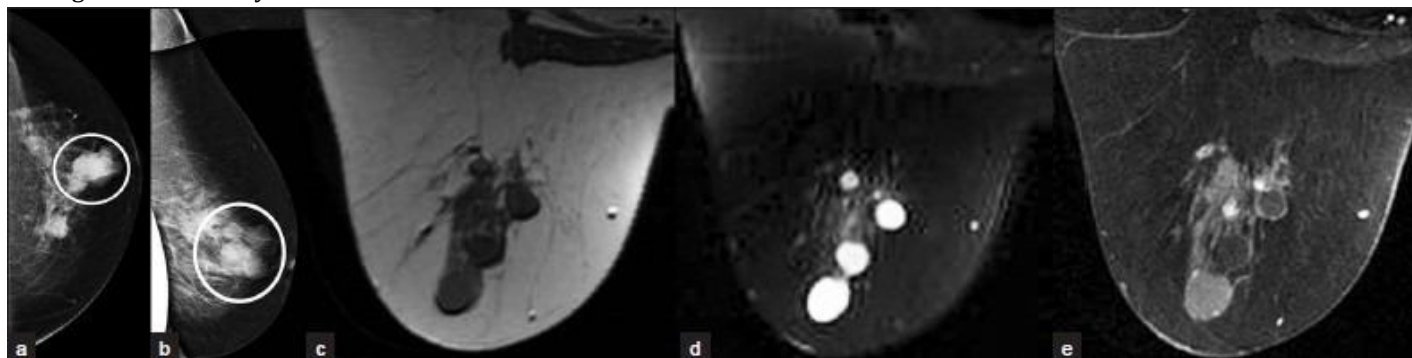


**Figure 3**

Simple cyst. (a) CC and (b) ML views of the left breast demonstrate several well-circumscribed round/oval masses nearly isodense to the parenchyma (circles). MR images demonstrate these masses to be (c) hypointense on T1WI, (d) hyperintense on T2WI, and (e) nonenhancing.

A *fibroadenoma* [Figure 4] is the second-most common benign breast lesion behind the simple cyst. On MRI, it is a focus or mass of enhancement with benign morphologic characteristics (without spiculations or microlobulations), nonenhancing dark internal septations, and follows a Type-I kinetics curve.

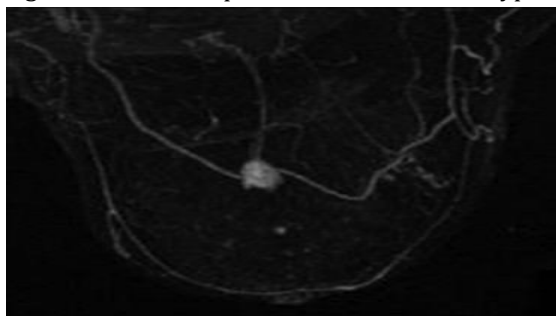


**Figure 4**

Fibroadenoma. MIP image demonstrates an enhancing mass without spiculations or microlobulations.

An *intramammary lymph node* appears as an intraparenchymal breast mass with an eccentric fatty hilum. It is often small, oval, and smoothly margined. Though it may be located anywhere in the breast, it is more commonly located in the upper-outer quadrant. MRI characteristics include a high-signal fatty hilum on T1W images, high signal on T2W images, and rapid, intense enhancement with contrast. On mammography, an intramammary lymph node may have a reniform or lobulated mass with a fatty hilum or notch. On ultrasound, it is a hypoechoic reniform mass with an echogenic fatty hilum.

Common malignant lesions

Malignant breast lesions can also have a variable appearance on MRI. These lesions often show low-signal intensity on T1W imaging, and low or moderate signal intensity on T2W imaging. Malignant lesions enhance with variable enhancement kinetics, as above. They often show restricted diffusion.

Ductal Carcinoma *in situ* (DCIS) is a neoplasm of variable grade and may not be visualized on MRI. It may have non-mass-like enhancement that can be clumped, ductal, linear, or segmental in shape. Enhancement kinetics are not useful because this lesion shows slow initial enhancement without washout (Type-I curve).

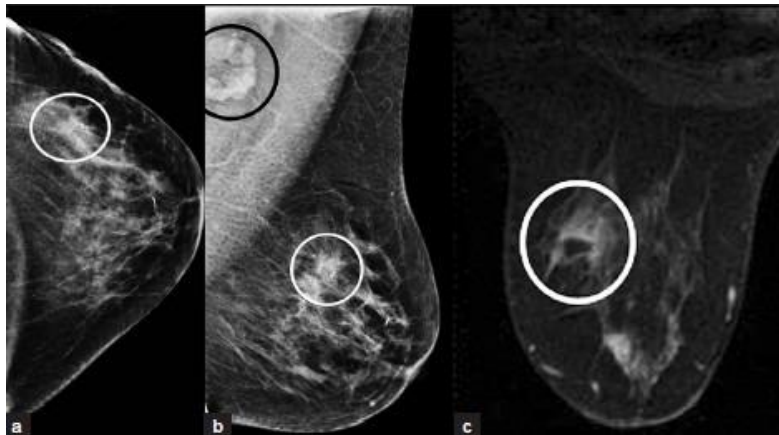


Figure 5

DCIS. (a) CC and (b) MLO views of left breast with microcalcifications (not well projected), soft tissue density, and biopsy clip in the outer aspect (white ovals). Axillary lymphadenopathy (black oval) is noted on the MLO view. (c) Post-contrast MR image of left breast showing clumped non-masslike enhancement in the outer aspect (oval). Note central low-signal artifact from a biopsy tract.

*Invasive ductal carcinoma* is the most common primary malignant tumor of the breast. MRI demonstrates an irregularly shaped, spiculated mass, with rim or heterogeneous enhancement. These lesions often display Type-II or Type-III washout curves. However, morphology is always more significant a tool for diagnosis than kinetic curve assessment.

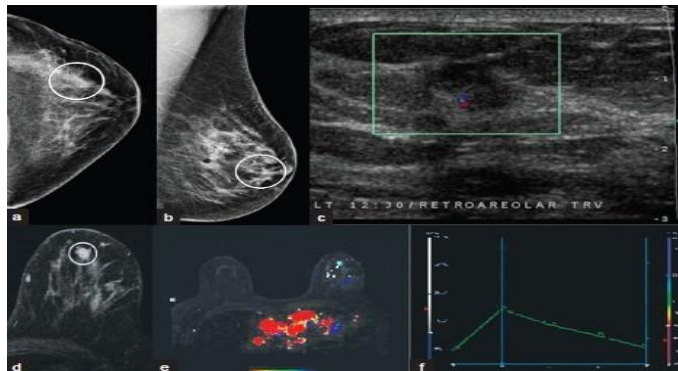
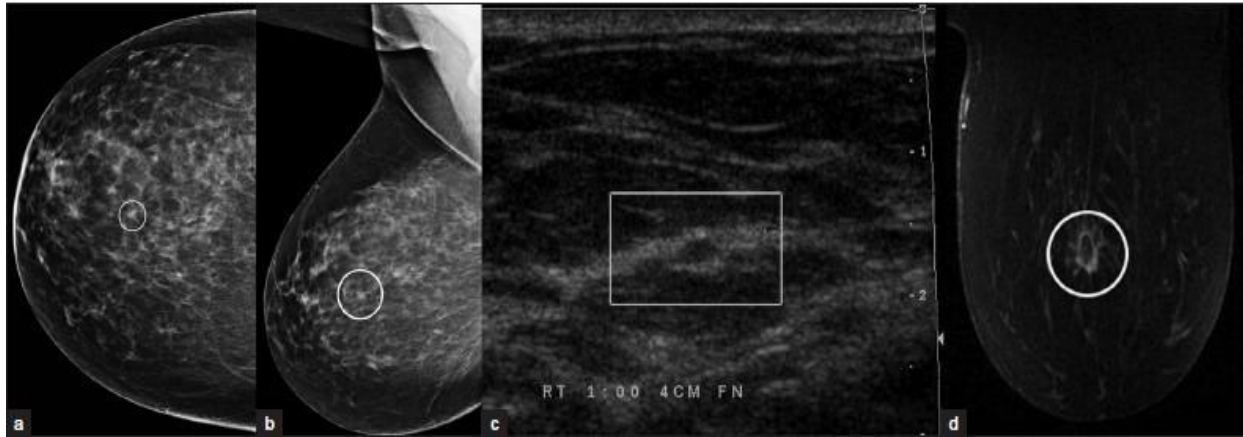


Figure 6

Invasive ductal carcinoma. (a) CC and (b) MLO views of the left breast demonstrate an irregular mass with indistinct spiculated margins (white ovals) (c) Ultrasound image demonstrates a taller-than-wide hypoechoic irregular mass with indistinct margins. (d) Postcontrast MR images demonstrate heterogeneous enhancement of the mass (oval). Note (e) the color map overlay and (f) type III enhancement curve of the mass.

*Invasive lobular carcinoma* comprises about 10% of all breast carcinomas. It is very difficult to detect mammographically due to an insidious growth pattern and a density equal or less than that of normal breast tissue. Both mammography and ultrasound often underestimate the lesion size, which has implications for staging and treatment. MRI has a higher sensitivity for lobular carcinoma and can more accurately assess the lesion size.[8] It commonly appears as multicentric/multifocal, spiculated focus or mass with architectural distortion. Enhancement can be asymmetric and nonmasslike in a ductal, segmental, regional, or diffuse pattern.



**Figure 7**

Invasive lobular carcinoma. (a) CC and (b) MLO views of the right breast demonstrate a spiculated focus (ovals). (c) Ultrasound image demonstrates a hypoechoic lesion with echogenic rim. (d) Postcontrast MR image demonstrates rim-enhancement of the mass with extension of enhancement within adjacent tissue (oval).

In DCE-MRI, when a contrast agent is administered, different enhancement kinetics can be identified. A slow, continuous enhancement curve (type I) is attributed to a benign lesion. A medium or strong enhancement followed by a plateau or persistent enhancement (type II) is indicative of either a benign or malignant lesion. A fast initial enhancement and wash-out (type III) is typically seen in malignancies, due to increased vascular permeability, density, and interstitial fluid (14). According to several studies and recommendations in the revised BI-RADS lexicon, the combination of functional and morphological information is necessary for the optimal evaluation of breast lesions (4).

The ACR recommends that the morphology of lesions should be reported using standardised BI-RADS descriptors. Larger tumour size, spiculate or irregular margins and shape, a wash-out curve or heterogeneous enhancement are descriptors that most strongly indicate malignancy (4, 15-17). In contrast, typically benign morphological features include round or oval shape, circumscribed margins, dark septa, and homogeneous slow-to-medium/persistent enhancement (15, 18). With 97-100% of histologically confirmed benign lesions showing smooth margins, this feature has the highest predictive value for the presence of a benign lesion (18, 19). For non-mass-like enhancement, benign lesion criteria include cystic changes, and diffuse bilateral enhancement (20). According to a modified interpretation scheme, a lesion should be assigned a BI-RADS category 4 if both shape and margin are suspicious but enhancement kinetics suggest a benign lesion, or if lesion shape and margin are both non-suspicious but a wash-out is observed (21). Although DCE-MRI aids in

the differentiation between benign and malignant breast lesions, needle biopsy is still generally recommended for newly diagnosed BI-RADS 4 or 5 lesions.

When cancer is detected, DCE-MRI can be used for simultaneous assessment of disease extent, satellite lesions, and multifocal, multicentric, and bilateral disease. DCE-MRI seems particularly more useful than mammography and ultrasound for evaluating invasive lobular cancer (ILC), ductal carcinoma in situ (DCIS), multifocal/multicentric disease, and lesions with a suspected associated extensive intraductal component (EIC; Fig. 1) (22, 23). If additional suspicious lesions are found on preoperative MRI, histopathological verification before alteration of treatment strategies is mandatory. Although DCE-MRI improves the pre-treatment assessment of disease, it remains controversial whether or not it improves overall or disease-free survival (24).

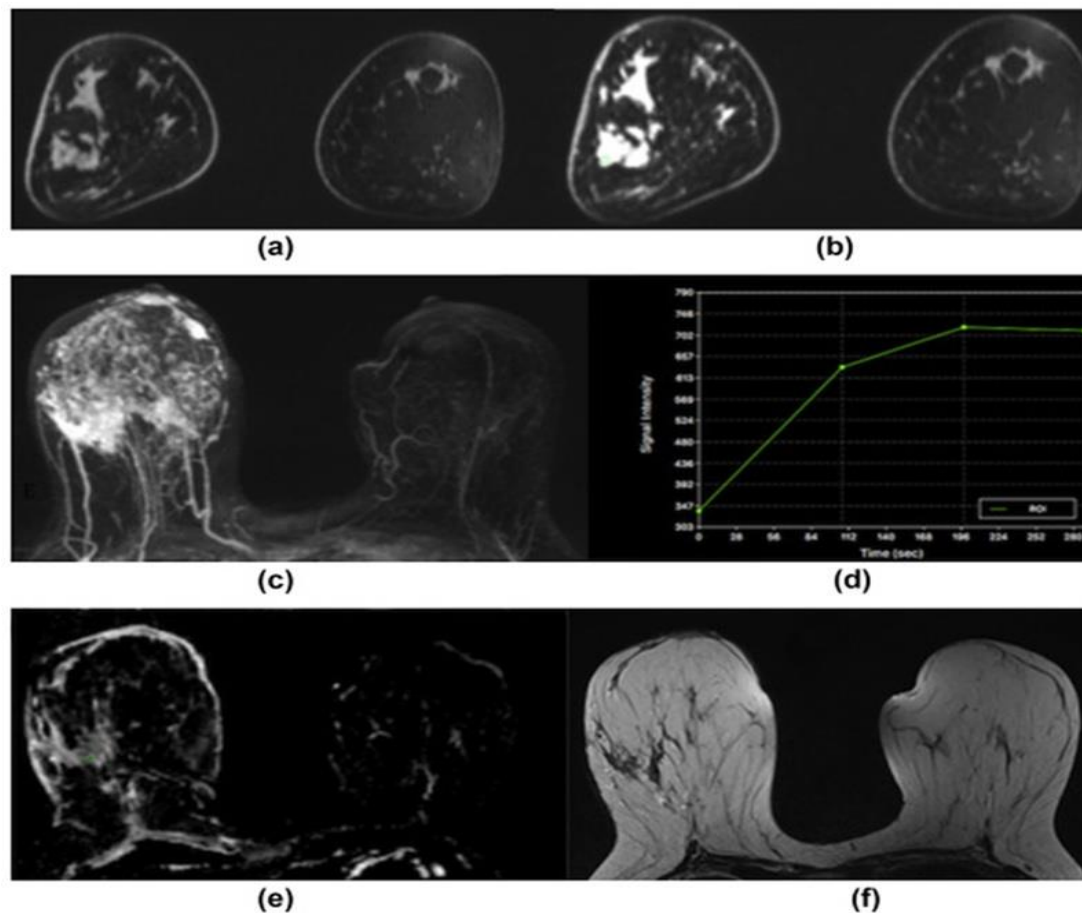


**Figure 8**

Invasive ductal carcinoma grade 3 in the right breast in a 40-year-old woman at 3 T. (a) Unenhanced, (b) contrast-enhanced, and (c) maximum-intensity-projection DCE-MRI images showing irregular-shaped and margined masses with extensive associated non-mass enhancement indicative of an extensive intraductal component in different quadrants of the right breast. (d) The index lesion demonstrates fast initial enhancement and a washout delayed phase (Type 3 curve). (e) On DWI with ADC mapping there is restricted diffusivity with decreased ADC values ( $0.971 \times 10^{-3} \text{ mm}^2/\text{s}$ ) associated with malignancy. (f) On the T2-weighted non-fat-saturated image there is associated peritumoural/paraseptal oedema indicative of lymphangiosarcomatosa.

DCE-MRI can be performed at different field strengths from 1.5 to 7 T, and so far has yielded excellent results for the assessment of breast cancer, with a sensitivity of up to 99% and a specificity of up to 97%

(9, 14, 25, 26). Its relatively high rate of false-positives occurs due to a significant overlap between benign and malignant lesions, and may result in additional work-up and unnecessary breast biopsies. To reduce background enhancement of normal parenchyma and hence the rate of false-positives, DCE-MRI should ideally be performed in the second week of the menstrual cycle (27).

Ways to improve DCE-MRI include the utilisation of high-resolution protocols, enabling a more accurate assessment of tumour morphology and neoangiogenesis. Its diagnostic value can be further improved by parallel imaging techniques and higher field strengths leading to increased spatial and temporal resolution; thus breast MRI is increasingly moving towards 3 T (26, 28) and possibly even higher field strengths.

With the implementation of high-resolution DCE-MRI protocols at 3 or 7 T, more sophisticated approaches than the above-described BI-RADS recommendations have been explored. A prime example is semi-quantitative curve type analysis by means of pharmacokinetic modelling. MRI pharmacokinetic models allow the quantification of the exchange of contrast agent between the intravascular and the interstitial space, thereby capturing tumour blood flow, microvasculature, and capillary permeability. The Tofts two-compartment model is the most commonly used model and provides MRI pharmacokinetic parameters of  $K_{trans}$ ,  $K_{ep}$ , and  $V_e$  (%) from post-processed DCE-MRI (29, 30).  $K_{trans}$  is related to the rate of contrast agent uptake into tumour from blood;  $K_{ep}$  is the rate of contrast agent transport from tumor to blood;  $V_e$  (%) is the leakage of fractional volume from the extravascular extracellular space into the plasma compartment (29, 30).  $K_{trans} > 0.25/\text{min}$  and  $K_{ep} > 1/\text{min}$  are associated with malignancy, and therefore, have been suggested as parameters to aid in the differentiation between benign and malignant breast tumours (31–33). Li *et al.* found that  $K_{ep}$  might be the best indicator when discriminating malignant from benign breast lesions (34) and Huang *et al.* showed that the application of a cut-off for  $K_{trans}$  values can obviate unnecessary biopsies in lesions (35). In addition, pharmacokinetic MRI parameters have been investigated for differentiation of different breast cancer subtypes. Yim *et al.* found that  $V_e$  values were significantly lower in tumors with high tumor-to-stroma ratio, whereas  $K_{ep}$  values were significantly lower in breast cancers with dominant collagen type and higher in cancers with high nuclear grade (36). Pharmacokinetic MRI parameters have also been proven useful in patients who have undergone neoadjuvant chemotherapy for response assessment. Data from a recent meta-analysis from Marinovich *et al.* indicate that  $K_{trans}$  is an earlier predictor of response and outperforms standard measures such as tumor size (37, 38).

Although results for pharmacokinetic modelling in breast MRI are promising, a seamless implementation in clinical practice is challenging. Several parameters, e.g., the pre-contrast T1 relaxation times of the tumour/tissue and the arterial input function, have to be known and can influence the results. In addition, the use of different aging techniques and modelling algorithms may also lead to varying results of quantitative measurements. More data and rigorous technique are necessary to employ the potential of quantitative DCE-MRI.

#### ULTRA-HIGH FIELD MRI

Ultra-high field MRI at 7 T has become available recently, providing a further increase in intrinsic signal-to-noise ratio, which can then be translated into higher spatial and temporal resolution (26). MRI at ultra-high field strength has its limitations, such as longer T1 relaxation times, shorter T2 decay time, greater specific absorption rate (SAR), and increased transmit field inhomogeneity, resulting in reduced image quality (39); however, according to several recent studies, these challenges in breast MRI at 7 T could be overcome (Fig. 9) (3, 39). In the first clinical study, Pinker *et al.* found that bilateral breast MRI at 7 T is feasible and offers high image quality, with a diagnostic accuracy of 96.6% (3). As the acquisition of T2-weighted images is limited at 7 T due to greater SAR, Bogner *et al.* developed a DWI protocol for 7 T MRI, which yields apparent diffusion coefficient (ADC) maps and additional T2-weighted images (40). Nevertheless, MRI at ultra-high field strength remains challenging and is still not routinely used.

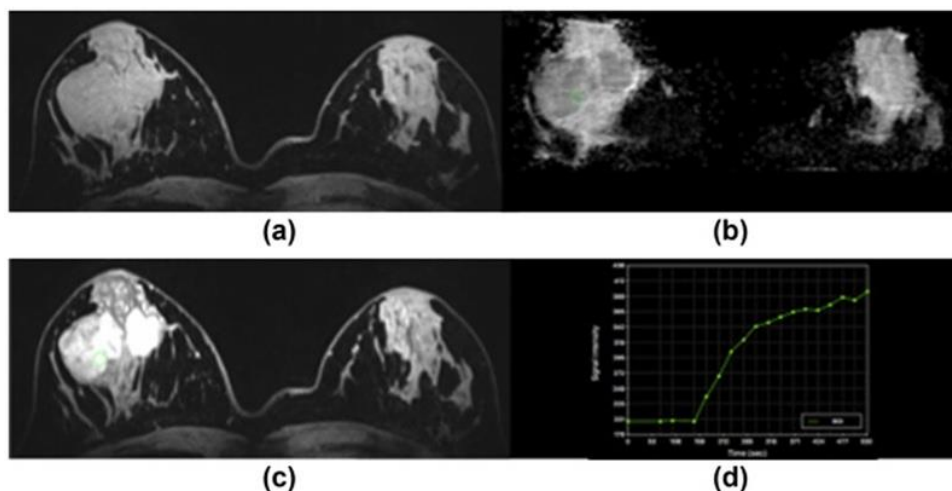


**Figure 9.**

Fibroadenoma in the right breast in a 23-year-old woman at 7 T. (a) Unenhanced and (c) contrast-enhanced DCE-MRI images show that there are two oval masses with partly irregular margins centrally in the right breast. The medial lesion demonstrates a homogeneous and the lateral mass a heterogeneous internal enhancement pattern, but also non-enhancing septa. (d) Both lesions demonstrate an initial medium and then persistent enhancement. (b) On DWI, there is no restricted diffusivity with ADC values of  $1.547 \times 10^{-3} \text{ mm}^2/\text{s}$ . MP MRI of the breast accurately classified the lesion as BI-RADS 2 benign.

Although the utility of breast MRI for screening of high-risk patients is well established (1, 2, 41), its high cost and longer examination time compared with mammography may limit its widespread use for screening of patients at average risk of breast cancer (42). Therefore, several recent studies investigated abbreviated and ultra-fast MRI protocols for breast cancer screening and diagnosis. Abbreviated protocols consisting, for instance, of a pre-contrast and an early post-contrast T1-weighted sequence (43–47), or, alternatively, a high-resolution ultrafast dynamic imaging protocol (48), were found suitable to diagnose breast cancer with high accuracy. In a recent study, Mango *et al.* investigated the diagnostic value of an abbreviated protocol consisting of a pre-contrast T1-weighted sequence and an initial postcontrast T1-weighted sequence, both with fat saturation in 100 cancers. Readers interpreted the first post-contrast T1-weighted image, post-processed subtracted first post-contrast image, and maximum intensity projection images (43). Mean sensitivities of 93–96% for each sequence were reached, at a mean interpretation time of 44 seconds. In previous studies, abbreviated protocols with a total scan time of 3–10 minutes were investigated. The authors concluded that an abbreviated examination could translate into decreased cost and make breast MRI a more accessible modality. Hence, substantially shortened MRI protocols are feasible for breast cancer detection, and after refinement might be implemented into clinical routine in the future. Nevertheless, prospective trials with larger patient numbers are warranted to evaluate the true value of abbreviated MRI for breast cancer screening. Unfortunately, an inherent limitation of DCE-MRI is the fact that it can provide only limited functional information, and still yields too many false-positive findings. In addition, recent controversy about gadolinium-containing contrast agents and recommendations to use them only when unenhanced MRI cannot obtain essential information emphasise the need for additional unenhanced MRI parameters.

#### BEYOND CONTRAST

During their development, cancers acquire multiple functional capabilities, known as the hallmarks of cancer, which to some extent can be evaluated using MRI (8). While DCE-MRI provides excellent information on tumour morphology and limited data on neoangiogenesis, not all benign and malignant lesions can be differentiated using this method alone. To assess additional functional tumour information and increase

specificity while preserving sensitivity, other MRI parameters, such as those derived from DWI and MRSI, have been developed and introduced into the clinical routine.

#### DWI and ADC mapping

In DWI, the random movement of water molecules in body tissue, i.e., Brownian motion, can be visualised and quantified by calculating the ADC. Malignancies typically show restricted water molecule diffusivity with high signal on DWI and lower signal on ADC maps due to increased cell density, which leads to compression of extracellular space, and microstructural changes. Technical developments, such as parallel imaging, better gradient systems, and multi-channel coils have overcome earlier limitations, such as susceptibility and motion artefacts, and DWI is now an essential part of oncological imaging (49). DWI can be easily implemented in every breast MRI protocol without substantially increasing the total scan time. The optimal choice of b-values remains controversial, with a recent meta-analysis recommending b-values of 0 and 1000 s/mm<sup>2</sup> (1.5 T) (50), while other studies found the optimal quality of DWI to be b-values of 50 and 850 s/mm<sup>2</sup> (3 T) (51). Although DWI is valuable, it should not be used as a standalone parameter as it detects significantly fewer malignancies compared with DCE-MRI. Conversely, adding DWI to DCE-MRI provides higher specificity (75–84%) than DCE-MRI alone (67–(52)72%), as well as additional functional information (53). As DWI is easy to perform and provides important functional information, it should be part of a routine breast MRI protocol. DWI has been found to be potentially useful as a non-invasive biomarker for the assessment of tumour subtype, receptor status, aggressiveness, tumour grade, and recurrence scores. For instance, ADC values were shown to be higher in ER-negative than in ER-positive tumours, while human epidermal growth factor receptor (HER2)-enriched tumours had the highest ADC values. ADC values also differed significantly between DCIS and invasive cancers as well as grades (52, 54, 55). In addition, DWI can be used for the monitoring of treatment response, as changes in ADC values occur earlier than changes in lesion size or vascularisation (56).

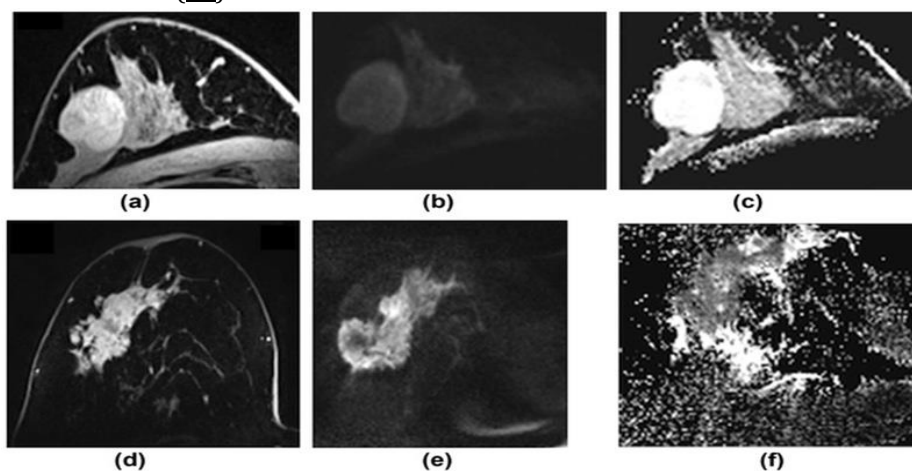


**Figure 10.**

Comparison of a benign and malignant breast tumour on DWI with ADC mapping at 7 T. (a) On DCE-MRI, the benign lesion, which is a fibroadenoma, is oval, circumscribed, and shows non-enhancing septa. (b) On the high b-value (b=850) images the lesion is hyperintense due to a T2-shinethrough, but on the ADC map (c) there is no restricted diffusivity with ADC values of  $2.226 \times 10^{-3} \text{ mm}^2/\text{s}$ . (d) On DCE-MRI, the malignant lesion (invasive ductal carcinoma grade 3) is irregular shaped and marginated and shows heterogeneous enhancement. (e) On the high b-value (b=850) images, the lesion is hyperintense, and (f) on the ADC map, there is restricted diffusivity (i.e., hyperintense) with ADC values of  $0.728 \times 10^{-3} \text{ mm}^2/\text{s}$ .

#### Emerging techniques

MP MRI allows the non-invasive visualization of different aspects of tumour biology. New MRI parameters, such as <sup>23</sup>Na-MRI, <sup>31</sup>P-MRSI, <sup>1</sup>H-lipid MRSI, CEST, BOLD, and hyperpolarised MRI, as well as advanced DWI

approaches and hybrid imaging methods, such as positron-emission tomography (PET)/MRI, have been developed to further improve this imaging method (74–76).

$^{23}\text{Na}$ -MRI has been introduced to provide information on the physiological and biochemical state of the tissue, with sodium concentration being an indicator of cellular metabolic integrity and ion haemostasis. The breakdown of cell membranes and failure of the  $\text{Na}^+/\text{K}^+$  ATPase pump leads to increased sodium levels, a sensitive marker for malignancy (77).  $^{23}\text{Na}$ -MRI benefits from ultra-high field strength and aids in the differentiation of benign and malignant breast tumours with complementary information about pathophysiological changes, with a diagnostic accuracy similar to DWI (78).

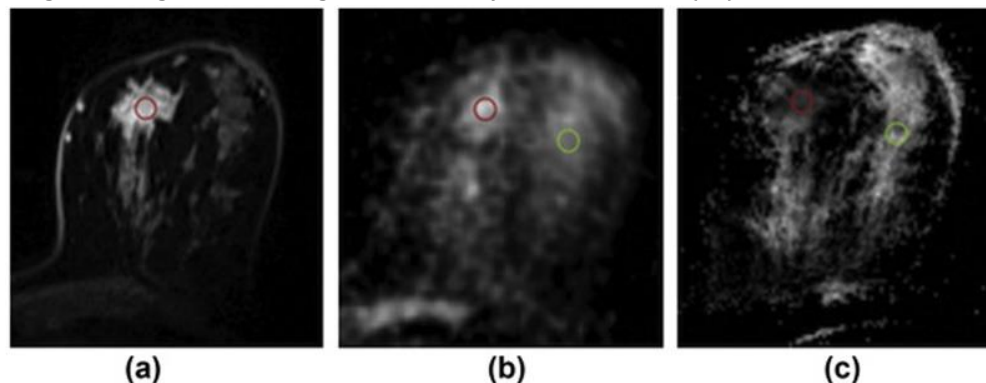


**Figure 11**

Invasive ductal carcinoma (grade 3) in the left breast of a 49-year-old female patient at 7 T. (a) Axial contrast-enhanced T1-weighted, fat-saturated, time-resolved angiography with stochastic trajectories MRI image shows initial strong contrast enhancement. (b) Corresponding axial Na-MRI image shows higher signal intensity in tumour tissue than the surrounding glandular tissue. (c) ADC map shows low ADC values inside the lesion (red region of interests [ROIs] are placed in lesions, and green ROIs are placed in healthy glandular tissue; 78). Reprinted with permission from: Zaric O, Pinker K, Zbyn S, *et al.* Quantitative sodium MR imaging at 7 T: initial results and comparison with diffusion-weighted imaging in patients with breast tumours. *Radiology*. 2016;280(1):39-48.

$^{31}\text{P}$ -MRSI measures membrane phospholipid metabolism, which serves as a biomarker for tumour progression and therapy response. Breast cancers typically show elevated levels of phosphocholine and phosphoethanolamine compared to healthy breast tissue. This method also benefits from higher field strengths and is expected to be a useful imaging tool for breast cancer diagnosis, staging, and therapy response (79, 80). Currently, the clinical use of  $^{31}\text{P}$ -MRSI is limited, as specific coils are necessary and ultra-high field scanners are not widely available.

$^1\text{H}$ -lipid MRSI measures lipid metabolism, which may serve as a biomarker for breast cancer diagnosis and therapy response. Some *ex vivo* NMR and *in vivo* MRSI studies have shown differences in fat between malignant, benign, and normal fibroglandular tissue with lower methylene ( $-\text{CH}_2-$ ) lipid peak intensities at 1.3 ppm in breast cancer at 1.5 T (81, 82). Due to the possibility of high field clinical scanners at 3 T and higher, and consequently, the increased signal-to-noise ratio, it is expected that an even broader spectrum of lipid metabolites for breast cancer diagnosis and molecular subtyping can be imaged. A recent study in patients with breast lesions demonstrated the detection of polyunsaturated fatty acids within the adipose tissue lipid  $^1\text{H}$ -MRSI; this information may be valuable as polyunsaturated fatty acids, apart from being a marker of obesity, is also related to an increased risk in breast cancer (83). The clinical use of  $^1\text{H}$ -lipid MRSI is gaining attention in breast cancer and methods to collect lipid spectrum spatially over the whole breasts with the availability of multi-channel phased array coils and high field strength clinical magnets are being developed with the potential to further provide valuable insights into tumour biology. CEST can differentiate tumour from healthy tissue through the amide proton transfer effect (ATP), providing information about the association of protons with mobile proteins (84, 85). A recent feasibility study at 3 T indicated similar lesion

detection and differentiation between ATP CEST MRI using contrast generated by endogenous molecules and DCE-MRI (86). Other CEST contrasts besides ATP are currently being investigated in animal studies. Dynamic CEST after the administration of glucose (glucoCEST) enables the evaluation of glycolysis (74). Amide, amine, and aliphatic CEST (aaaCEST) allows the differentiation of areas of apoptosis/necrosis from actively progressing cancer (87).

BOLD MRI, on the other hand, depicts tissue hypoxia, which is typically associated with tumour progression, recurrence, treatment resistance, and metastasis. This technique might therefore serve as a valuable imaging biomarker for breast cancer diagnosis and treatment response in the future (75, 88).

HP MRI is one of the most recent techniques in molecular imaging, allowing a non-invasive investigation of metabolic pathways by using contrast agents that have been “hyperpolarised”. In conventional MRI nuclear spins are polarised on the order of a few parts per million, whereas in HP MRI, spins reach near-unity polarisation, resulting in a substantially increased signal intensity (89). HP probes are injected into living organisms and their metabolism can be visualised in real-time with chemical shift imaging. Recent animal studies have demonstrated that HP MRI enables the differentiation of benign and malignant tumours through real-time measurement of the transformation of  $^{13}\text{C}$  pyruvate into lactate and alanine (90, 91). Other probes to visualise different metabolic pathways, such as necrosis ( $^{13}\text{C}$  fumarate), and glutamine metabolism ( $^{13}\text{C}$  glutamine) are still under investigation (92). Although, to date, its future clinical role is unclear, several pre-clinical studies indicate that this technique might be valuable for the detection of breast cancer.

In addition to simple isotropic DWI model, several advanced DWI approaches are currently under investigation, such as diffusion tensor imaging (DTI), intravoxel incoherent motion (IVIM), and diffusion kurtosis imaging (DKI). DTI is an extension of DWI and provides detailed information about structural anisotropy. Whereas DWI can only capture molecular movements along the direction of the gradient, diffusion is truly a three-dimensional, anisotropic process, which can be captured with DTI and thus subtle micro-anatomical tissue alterations can be visualised; however, a clear incremental value compared with conventional ADC imaging has yet to be demonstrated (93, 94), with background parenchymal enhancement having a significant influence on primary diffusion coefficient as measured from DTI in control subjects. In contrast, microvascularity can be derived using the DWI-derived IVIM, thus enabling the separation and visualisation of perfusion and diffusion components that are combined in standard DWI signal in breast cancer diagnosis (95)

#### FURTHER BEYOND

##### Predictive and prognostic

MRI has a high predictive and prognostic value that has been demonstrated in multiple previous studies. A smooth margin of breast cancer in DCE-MRI proved to be predictive for positive lymph nodes, large tumour size, and low oestrogen receptor (ER) expression (96-100). Conversely, MR BI-RADS descriptors “skin thickening” and “internal enhancement” were found to be significantly associated with lymph node metastases, one of the most important prognostic factors in breast cancer (101,102). Prepectoral oedema also proved to be a strong prognostic indicator for lymphatic metastases, as well as high tumour grading (103). A very recent study suggested that heterogeneous enhancement of tumour-adjacent parenchyma is associated with tumour necrosis pathways and poor survival (104). In triple-negative (TN) cancers, peritumoural oedema has been associated with decreased recurrence-free survival, while central tumour necrosis and irregular mass on DCE-MRI were found to be prognostic factors for failure of neoadjuvant chemotherapy (105).

Several recent studies suggested that also DWI has great prognostic potential, as ADC values were found to predict tumour aggressiveness (106, 107). ADC values were also found to serve as prognostic factors for the presence of distant metastases at 3 years (108).

Established functional MRI parameters, such as DWI and MRSI, as well as emerging techniques, such as BOLD, are currently investigated as early biomarkers for response to neoadjuvant chemotherapy, as metabolic alterations seem to occur earlier than morphological changes, with promising results (56, 61).

### Radiogenomics

The discovery that breast cancer is a genetic disease has had substantial implications on how to treat it. It is now crucial to develop strategies that target specific genetic features of a malignant lesion, rather than employing a one-size-fits-all approach. Although well-established MRI factors, such as histological type, tumour size, grade, and receptor status, remain of great prognostic importance, these conventional approaches cannot fully cover the heterogeneity of breast cancer. Gene-expression profiling has revolutionised breast cancer classifications, and the traditional classifications based on immunohistochemistry (IHC) have been replaced by molecular subtypes. The Cancer Genome Atlas (TCGA) Network has defined four intrinsic molecular subtypes for the classification of breast cancer by extensive profiling at the DNA, microRNA, and protein levels: luminal A (ER- or progesterone [PR]-positive and HER2-negative), luminal B (ER- or PR-positive and HER2-positive), HER2-enriched (ER- and PR-negative and HER2-positive), and TN/basal-like (ER-, PR-, and HER2-negative) (109, 110). These subtypes show variations according to age, race, and menopausal status, and are not equally distributed among breast cancer patients (109). More importantly, they have distinct prognoses and outcomes, allowing different systemic therapy recommendations to be made based on subtype classification (111). Unfortunately, subtype classification is limited as there is no low-cost genetic testing readily available. Moreover, molecular subtypes derived from IHC surrogates have been shown to be less robust for predicting patient outcomes; however, with substantial advances in medical imaging techniques, image analysis, and the development of high-throughput methods to extract and correlate multiple imaging parameters with genomic data, a new direction has entered the clinical area and is rapidly evolving. Radiogenomics is a novel non-invasive approach that aims to associate imaging findings with molecular subtypes, gene mutations, and other genome-related features of cancers. To date, the field of radiogenomics in breast imaging is dominated by MRI with recent attempts to also include functional parameters such as DWI. So far, radiogenomics of breast cancer has focused incorporating genomic data from either breast cancer molecular subtypes, individual genomic signatures, or clinically used recurrence scores (OncotypeDx, Genomic Health, CA, USA; MammaPrint, Agendia, CA, USA; Mammostrat, Clariant Diagnostic Services, CA, USA; PAM50/Prosigna, NanoString, WA, USA).

For instance, it has been demonstrated that the luminal B subtype, having a worse prognosis than luminal A subtypes, is associated with a higher enhancement ratio of tumour to normal breast parenchyma in DCE-MRI (112, 113). At the same time, breast cancers with HER2 overexpression tend to present with fast initial enhancement or wash-out (114). A circumscribed margin has been described to be associated with HER2-enriched subtypes, while multifocal/multicentric disease is more often found in HER2 or luminal B subtypes (115). In DWI, HER2-enriched cancers were demonstrated to have the highest ADC values, while luminal B, HER2-negative tumours had the lowest ADC values; these findings might be explained by increased neo-angiogenesis in HER2 subtypes (54, 116). Most triple-negative tumours are classified as basal-like, and were found to be associated with rim enhancement and high signal intensity on T2-weighted sequences (117). In attempts to develop imaging biomarkers as surrogates for genetic testing, several studies investigated the correlation of radiogenomics with molecular subtypes. Whereas Waugh *et al.* had only limited success (118), Grimm *et al.* found a strong association between the morphological, kinetic, and textural imaging features and both luminal A ( $p=0.0007$ ) and luminal B ( $p=0.0063$ ) subtypes (119). Li *et al.* investigated the performance of a classifier model for molecular subtyping and the computer-extracted tumour phenotypes were shown to distinguish between molecular prognostic indicators. Different investigators also evaluated radiogenomics for predicting the risk of recurrence (120–122) and found that there were significant associations between breast cancer MRI radiomics signatures and multigene assay recurrence scores.

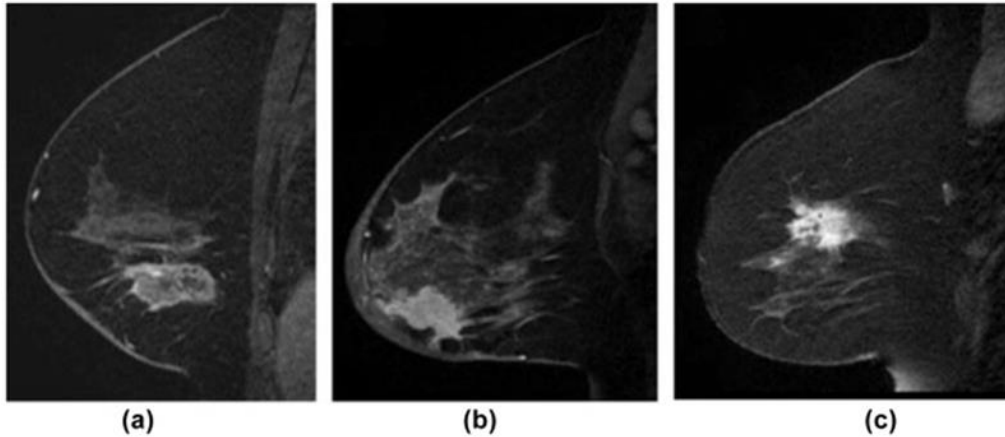


Figure 12

Radiogenomics. A machine-learning-based predictive model using image features extracted from MRI can distinguish invasive ductal carcinoma (IDC) subtypes based on some image features that are imperceptible to the eye. (a) Sagittal T1-weighted fat-suppressed post-contrast MRI of an ER and PR positive (ERPR+) invasive ductal carcinoma. (b) Sagittal T1-weighted fat-suppressed postcontrast MRI of an ERPR-/HER2 invasive ductal carcinoma. (c) Sagittal T1-weighted fat-suppressed post-contrast MRI of a triple-negative invasive ductal carcinoma [121]. Reprinted with permission from: Sutton EJ, Dashevsky BZ, Oh JH, et al. Breast cancer molecular subtype classifier that incorporates MRI. *J Magn Reson Imaging*. 2016;44(1):122-129.

Radiogenomics is a promising field with the aim to pair information derived from genetic tests and diagnostic imaging, but is still limited by heterogeneity of datasets by different institutions and challenges in genetic testing. Larger prospective studies are warranted to meaningfully implement radiogenomics in the clinical routine in the future.

#### CONCLUSIONS

DCE-MRI has been an essential method in the field of breast imaging, providing excellent morphological and to some extent functional information, with multiple clinical indications. Nevertheless, there are several improvements being investigated. Abbreviated and ultra-fast MRI protocols are being investigated to save costs and hence make breast cancer screening with MRI more available for women. Moreover, with advances in medical imaging techniques, image analysis, and the development of high-throughput methods to extract and correlate multiple imaging parameters with genomic data, the field of radiogenomics has emerged and aims to correlate imaging phenotypes with genomic cancer characteristics to provide deeper insights in pathologic processes. A paradigm shift establishing advanced morpho-functional imaging with MRI and the implementation of radiogenomics is expected to further improve the diagnosis, prediction, and prognosis of breast cancer, ultimately realising the goal of precision medicine.

#### References:

1. Sardanelli F, Boetes C, Borisch B, et al. Magnetic resonance imaging of the breast: recommendations from the EUSOMA working group. *Eur J Cancer*. 2010;46(8): 1296–1316. [PubMed] [Google Scholar]
2. Mann RM, Balleyguier C, Baltzer PA, et al. Breast MRI: EUSOBI recommendations for women's information. *EurRadiol*. 2015. [PMC free article] [PubMed] [Google Scholar]
3. Pinker K, Bogner W, Baltzer P, et al. Clinical application of bilateral high temporal and spatial resolution dynamic contrast-enhanced MR imaging of the breast at 7 T. *EurRadiol*. 2014;24(4):913–920. [PubMed] [Google Scholar]
4. Pinker-Domenig K, Bogner W, Gruber S, et al. High resolution MRI of the breast at 3 T: which BI-RADS(R) descriptors are most strongly associated with the diagnosis of breast cancer? *EurRadiol*. 2012;22(2):322–330. [PubMed] [Google Scholar]
5. Morris EA. Diagnostic breast MR imaging: current status and future directions. *Radiol Clin North Am*. 2007;45(5):863–880, vii. [PubMed] [Google Scholar]
6. Morrow M, Waters J, Morris E. MRI for breast cancer screening, diagnosis, and treatment. *Lancet*. 2011;378(9805):1804–1811. [PubMed] [Google Scholar]

7. Hanahan D, Weinberg RA. The hallmarks of cancer. *Cell*. 2000;100(1):57–70. [PubMed] [Google Scholar]
8. Hanahan D, Weinberg RA. Hallmarks of cancer: the next generation. *Cell*. 2011;144(5):646–674. [PubMed] [Google Scholar]
9. Pinker K, Grabner G, Bogner W, et al. A combined high temporal and high spatial resolution 3 Tesla MR imaging protocol for the assessment of breast lesions: initial results. *Invest Radiol*. 2009;44(9):553–558. [PubMed] [Google Scholar]
10. Folkman J Seminars in Medicine of the Beth Israel Hospital, Boston. Clinical applications of research on angiogenesis. *N Engl J Med*. 1995;333(26):1757–1763. [PubMed] [Google Scholar]
11. Pinker K, Bogner W, Baltzer P, et al. Clinical application of bilateral high temporal and spatial resolution dynamic contrast-enhanced magnetic resonance imaging of the breast at 7 T. *EurRadiol*. 2014;24(4):913–920. [PubMed] [Google Scholar]
12. Pinker-Domenig K, Bogner W, Gruber S, et al. High resolution MRI of the breast at 3 T: which BI-RADS(R) descriptors are most strongly associated with the diagnosis of breast cancer? *EurRadiol*. 2011. [PubMed] [Google Scholar]
13. D'Orsi CJ, Sickles EA, Mendelson EB, et al. ACR BI-RADS® Atlas, Imaging Reporting and Data System, 5th edn Reston, VA: American College of Radiology, 2013. [Google Scholar]
14. Helbich TH. Contrast-enhanced magnetic resonance imaging of the breast *Eur J Radiol*. 2000;34(3):208–219. [PubMed] [Google Scholar]
15. Gutierrez RL, DeMartini WB, Eby PR, Kurland BF, Peacock S, Lehman CD BI-RADS lesion characteristics predict likelihood of malignancy in breast MRI for masses but not for nonmasslike enhancement. *AJR Am J Roentgenol* 2009; 193(4):994–1000. [PubMed] [Google Scholar]
16. Wang LC, DeMartini WB, Partridge SC, Peacock S, Lehman CD. MRI-detected suspicious breast lesions: predictive values of kinetic features measured by computer-aided evaluation. *AJR Am J Roentgenol*. 2009;193(3):826–831. [PubMed] [Google Scholar]
17. Liberman L, Mason G, Morris EA, Dershaw DD. Does size matter? Positive predictive value of MRI-detected breast lesions as a function of lesion size. *AJR Am J Roentgenol*. 2006;186(2):426–430. [PubMed] [Google Scholar]
18. Nunes LW, Schnall, Siegelman ES, et al. Diagnostic performance characteristics of architectural features revealed by high spatial-resolution MR imaging of the breast. *AJR Am J Roentgenol*. 1997;169(2):409–415. [PubMed] [Google Scholar]
19. Szabo BK, Aspelin P, Wiberg MK, Bone B. Dynamic MR imaging of the breast Analysis of kinetic and morphologic diagnostic criteria. *Acta Radiol*. 2003;44(4):379–386. [PubMed] [Google Scholar]
20. Agrawal G, Su MY, Nalcioglu O, Feig SA, Chen JH. Significance of breast lesion descriptors in the ACR BI-RADS MRI lexicon. *Cancer*. 2009;115(7):1363–1380 [PMC free article] [PubMed] [Google Scholar]
21. Kuhl CK, Schild HH, Morakkabati N. Dynamic bilateral contrast-enhanced MR imaging of the breast: trade-off between spatial and temporal resolution. *Radiology* 2005;236(3):789–800. [PubMed] [Google Scholar]
22. Esserman L, Hylton N, Yassa L, Barclay J, Frankel S, Sickles E. Utility of magnetic resonance imaging in the management of breast cancer: evidence for improved preoperative staging. *J Clin Oncol*. 1999;17(1):110–119. [PubMed] [Google Scholar]
23. Mann RM, Loo CE, Wobbes T, et al. The impact of preoperative breast MRI on the re-excision rate in invasive lobular carcinoma of the breast. *Breast Cancer Res Treat*. 2010;119(2):415–422. [PubMed] [Google Scholar]
24. Ryu J, Park HS, Kim S, Kim JY, Park S, Kim SI. Preoperative magnetic resonance imaging and survival outcomes in T1-2 breast cancer patients who receive breast-conserving therapy. *J Breast Cancer*. 2016;19(4):423–428. [PMC free article] [PubMed] [Google Scholar]
25. Elsamaloty H, Elzawawi MS, Mohammad S, Herial N. Increasing accuracy of detection of breast cancer with 3-T MRI. *AJR Am J Roentgenol*. 2009;192(4):1142–1148. [PubMed] [Google Scholar]
26. Kuhl CK, Jost P, Morakkabati N, Zivanovic O, Schild HH, Gieseke J. Contrast-enhanced MR imaging of the breast at 3.0 and 1.5 T in the same patients: Initial experience. *Radiology*. 2006;239(3):666–676. [PubMed] [Google Scholar]
27. Macura KJ, Ouwerkerk R, Jacobs MA, Bluemke DA. Patterns of enhancement on breast MR images: interpretation and imaging pitfalls. *RadioGraphics*. 2006;26(6): 1719–1734; quiz 1719. [PMC free article] [PubMed] [Google Scholar]
28. Rahbar H, Partridge SC, DeMartini WB, Thursten B, Lehman CD. Clinical and technical considerations for high quality breast MRI at 3 Tesla. *J Magn Reson Imaging*. 2013;37(4):778–790. [PMC free article] [PubMed] [Google Scholar]
29. Tofts PS, Berkowitz B, Schnall. Quantitative analysis of dynamic Gd-DTPA enhancement in breast tumours using a permeability model. *Magn Reson Med*. 1995;33(4):564–568. [PubMed] [Google Scholar]
30. Tofts PS, Brix G, Buckley DL, et al. Estimating kinetic parameters from dynamic contrast-enhanced T(1)-weighted MRI of a diffusable tracer: standardized quantities and symbols. *J Magn Reson Imaging*. 1999;10(3):223–232. [PubMed] [Google Scholar]
31. Braman NM, Etesami M, Prasanna P, et al. Intratumoural and peritumoural radiomics for the pretreatment prediction of pathological complete response to neoadjuvant chemotherapy based on breast DCE-MRI. *Breast Cancer Res*. 2017;19(1):57. [PMC free article] [PubMed] [Google Scholar]
32. Rahbar H, Partridge SC. Multiparametric MR imaging of breast cancer. *Magn Reson Imaging Clin N Am*. 2016;24(1):223–238. [PMC free article] [PubMed] [Google Scholar]

33. Helbich TH, Roberts TP, Gossmann A, et al. Quantitative gadopentetate-enhanced MRI of breast tumours: testing of different analytic methods. *Magn Reson Med*. 2000;44(6):915–924. [PubMed] [Google Scholar]
34. Li L, Wang K, Sun X, et al. Parameters of dynamic contrast-enhanced MRI as imaging markers for angiogenesis and proliferation in human breast cancer. *Med Sci Monit*. 2015;21:376–382. [PMC free article] [PubMed] [Google Scholar]
35. Huang W, Tudorica LA, Li X, et al. Discrimination of benign and malignant breast lesions by using shutter-speed dynamic contrast-enhanced MR imaging. *Radiology*. 2011;261(2):394–403. [PMC free article] [PubMed] [Google Scholar]
36. Yim H, Kang DK, Jung YS, Jeon GS, Kim TH. Analysis of kinetic curve and model-based perfusion parameters on dynamic contrast enhanced MRI in breast cancer patients: correlations with dominant stroma type. *Magn Reson Imaging*. 2016;34(1 ):60–65. [PubMed] [Google Scholar]
37. Pinker K, Helbich TH, Morris EA. The potential of multiparametric MRI of the breast. *Br J Radiol*. 2016:20160715. [PMC free article] [PubMed] [Google Scholar]
38. Marinovich ML, Houssami N, Macaskill P, et al. Meta-analysis of magnetic resonance imaging in detecting residual breast cancer after neoadjuvant therapy. *J Natl Cancer Inst*. 2013;105(5):321–333. [PubMed] [Google Scholar]
39. Umutlu L, Maderwald S, Kraff O, et al. Dynamic contrast-enhanced breast MRI at 7 Tesla utilizing a single-loop coil: a feasibility trial. *AcadRadiol*. 2010;17(8):1050–1056. [PubMed] [Google Scholar]
40. Bogner W, Pinker K, Zaric O, et al. Bilateral diffusion-weighted MR imaging of breast tumours with submillimeter resolution using readout-segmented echo-planar imaging at 7 T. *Radiology*. 2015;274(1):74–84. [PubMed] [Google Scholar]
41. Saslow D, Boetes C, Burke W, et al. American Cancer Society guidelines for breast screening with MRI as an adjunct to mammography. *CA Cancer J Clin*. 2007;57(2):75–89. [PubMed] [Google Scholar]
42. Berg WA, Zhang Z, Lehrer D, et al. Detection of breast cancer with addition of annual screening ultrasound or a single screening MRI to mammography in women with elevated breast cancer risk. *JAMA*. 2012;307(13):1394–1404. [PMC free article] [PubMed] [Google Scholar]
43. Mango VL, Morris EA, David Dershaw D, et al. Abbreviated protocol for breast MRI: are multiple sequences needed for cancer detection? *Eur J Radiol*. 2015;84(1):65–70. [PubMed] [Google Scholar]
44. Grimm LJ, Soo MS, Yoon S, Kim C, Ghate SV, Johnson KS. Abbreviated screening protocol for breast MRI: a feasibility study. *AcadRadiol*. 2015;22(9):1157–1162. [PubMed] [Google Scholar]
45. Kuhl CK, Schrading S, Strobel K, Schild HH, Hilgers RD, Bieling HB. Abbreviated breast magnetic resonance imaging (MRI): first postcontrast subtracted images and maximum-intensity projection—a novel approach to breast cancer screening with MRI. *J Clin Oncol*. 2014;32(22):2304–2310. [PubMed] [Google Scholar]
46. Moschetta M, Telegrafo M, Rella L, Stabile lanora AA, Angelelli G. Abbreviated combined MR protocol: a new faster strategy for characterizing breast lesions. *Clin Breast Cancer*. 2016;16(3):207–211. [PubMed] [Google Scholar]
47. Harvey SC, Di Carlo PA, Lee B, Obadina E, Sippo D, Mullen L. An abbreviated protocol for high-risk screening breast MRI saves time and resources. *J Am Coll Radiol*. 2016;13(4):374–380. [PubMed] [Google Scholar]
48. Mann RM, Mus RD, van Zelst J, Geppert C, Karssemeijer N, Platel B. A novel approach to contrast-enhanced breast magnetic resonance imaging for screening: high-resolution ultrafast dynamic imaging. *Invest Radiol*. 2014;49(9):579–585. [PubMed] [Google Scholar]
49. Partridge SC, McDonald ES. Diffusion weighted magnetic resonance imaging of the breast: protocol optimization, interpretation, and clinical applications. *Magn Reson Imaging Clin N Am*. 2013;21(3):601–624. [PMC free article] [PubMed] [Google Scholar]
50. Dorrius, Dijkstra H, Oudkerk M, Sijens PE Effect of b value and pre-admission of contrast on diagnostic accuracy of 1.5-T breast DWI: a systematic review and meta-analysis. *EurRadiol*. 2014;24(11):2835–2847. [PubMed] [Google Scholar]
51. Bogner W, Gruber S, Pinker K, et al. Diffusion-weighted MR for differentiation of breast lesions at 3.0 T: how does selection of diffusion protocols affect diagnosis? *Radiology*. 2009;253(2):341–351. [PubMed] [Google Scholar]
52. Thakur SB, Durando M, Milans S, et al. Apparent diffusion coefficient in estrogen receptor-positive and axillary lymph node-negative breast cancers at 3 T MRI: a potential predictor for a validated prognostic gene expression profile. *J Magn Reson Imaging*. 2017;in press. [PMC free article] [PubMed] [Google Scholar]
53. Spick C, Pinker-Domenig K, Rudas M, Helbich TH, Baltzer PA. MRI-only lesions: application of diffusion-weighted imaging obviates unnecessary MR-guided breast biopsies. *EurRadiol*. 2014;24(6):1204–1210. [PubMed] [Google Scholar]
54. Martincich L, Deantoni V, Bertotto I, et al. Correlations between diffusion-weighted imaging and breast cancer biomarkers. *EurRadiol*. 2012;22(7):1519–1528. [PubMed] [Google Scholar]
55. Bickel H, Pinker-Domenig K, Bogner W, et al. Quantitative apparent diffusion coefficient as a noninvasive imaging biomarker for the differentiation of invasive breast cancer and ductal carcinoma in situ. *Invest Radiol*. 2015;50(2):95–100. [PubMed] [Google Scholar]
56. Park SH, Moon WK, Cho N, et al. Diffusion-weighted MR imaging: pretreatment prediction of response to neoadjuvant chemotherapy in patients with breast cancer. *Radiology*. 2010;257(1):56–63. [PubMed] [Google Scholar]

57. Bartella L, Huang W. Proton (1H) MR spectroscopy of the breast. *RadioGraphics*. 2007;27(Suppl. 1):S241–252. [PubMed] [Google Scholar]
58. Pinker K, Stadlbauer A, Bogner W, Gruber S, Helbich TH. Molecular imaging of cancer: MR spectroscopy and beyond. *Eur J Radiol*. 2012;81(3):566–577. [PubMed] [Google Scholar]
59. Gruber S, Debski BK, Pinker K, et al. Three-dimensional proton MR spectroscopic imaging at 3 T for the differentiation of benign and malignant breast lesions. *Radiology*. 2011;261(3):752–761. [PubMed] [Google Scholar]
60. Baltzer PA, Dietzel M. Breast lesions: diagnosis by using proton MR spectroscopy at 1.5 and 3.0 T—systematic review and meta-analysis. *Radiology*. 2013;267(3):735–746. [PubMed] [Google Scholar]
61. Jagannathan NR, Kumar M, Seenu V, et al. Evaluation of total choline from in-vivo volume localized proton MR spectroscopy and its response to neoadjuvant chemotherapy in locally advanced breast cancer. *Br J Cancer*. 2001;84(8):1016–1022. [PMC free article] [PubMed] [Google Scholar]
62. Meisamy S, Bolan PJ, Baker EH, et al. Neoadjuvant chemotherapy of locally advanced breast cancer: predicting response with in vivo (1)H MR spectroscopy—a pilot study at 4 T. *Radiology*. 2004;233(2):424–431. [PubMed] [Google Scholar]
63. Glunde K, Bhujwala ZM, Ronen SM. Choline metabolism in malignant transformation. *Nat Rev Cancer*. 2011;11(12):835–848. [PMC free article] [PubMed] [Google Scholar]
64. Aboagye EO, Bhujwala ZM. Malignant transformation alters membrane choline phospholipid metabolism of human mammary epithelial cells. *Cancer Res*. 1999;59(1):80–84. [PubMed] [Google Scholar]
65. Woodhams R, Matsunaga K, Iwabuchi K, et al. Diffusion-weighted imaging of malignant breast tumours. The usefulness of apparent diffusion coefficient (ADC) value and ADC map for the detection of malignant breast tumours and evaluation of cancer extension. *J Comput Assist Tomogr*. 2005;29(5):644–649. [PubMed] [Google Scholar]
66. Pinker K, Baltzer P, Bogner W, et al. Multiparametric MR imaging with high-resolution dynamic contrast-enhanced and diffusion-weighted imaging at 7 T improves the assessment of breast tumours: a feasibility study. *Radiology*. 2015;141905. [PubMed] [Google Scholar]
67. Pinker K, Bickel H, Helbich T, et al. Combined contrast enhanced magnetic resonance and diffusion weighted imaging reading adapted to the “Breast Imaging Reporting and Data System” for multiparametric 3 T imaging of breast lesions. *Eur Radiol*. 2013. [PubMed] [Google Scholar]
68. Marino MA, Clauser P, Woitek R, et al. A simple scoring system for breast MRI interpretation: does it compensate for reader experience? *Eur Radiol*. 2015. [PubMed] [Google Scholar]
69. Baltzer A, Dietzel M, Kaiser CG, Baltzer PA. Combined reading of contrast enhanced and diffusion weighted magnetic resonance imaging by using a simple sum score. *Eur Radiol*. 2016;26(3):884–891. [PubMed] [Google Scholar]
70. Dijkstra H, Dorrius, Wielema M, Pijnappel RM, Oudkerk M, Sijens PE. Quantitative DWI implemented after DCE-MRI yields increased specificity for BIRADS 3 and 4 breast lesions. *J Magn Reson Imaging*. 2016. [PubMed] [Google Scholar]
71. Aribal E, Asadov R, Ramazan A, Ugurlu MU, Kaya H. Multiparametric breast MRI with 3 T: effectivity of combination of contrast enhanced MRI, DWI and 1H single voxel spectroscopy in differentiation of Breast tumours. *Eur J Radiol*. 2016;85(5):979–986. [PubMed] [Google Scholar]
72. Pinker K, Bogner W, Baltzer P, et al. Improved diagnostic accuracy with multiparametric magnetic resonance imaging of the breast using dynamic contrast-enhanced magnetic resonance imaging, diffusion-weighted imaging, and 3-dimensional proton magnetic resonance spectroscopic imaging. *Invest Radiol*. 2014;49(6):421–430. [PubMed] [Google Scholar]
73. Schmitz AM, Veldhuis WB, Menke-Pluijmers MB, et al. Multiparametric MRI with dynamic contrast enhancement, diffusion-weighted imaging, and 31-phosphorus spectroscopy at 7 T for characterization of breast cancer. *Invest Radiol*. 2015;50(11):766–771. [PubMed] [Google Scholar]
74. Nasrallah FA, Pages G, Kuchel PW, Golay X, Chuang KH. Imaging brain deoxyglucose uptake and metabolism by glucoCEST MRI. *J Cereb Blood Flow Metab*. 2013;33(8):1270–1278. [PMC free article] [PubMed] [Google Scholar]
75. Rakow-Penner R, Daniel B, Glover GH. Detecting blood oxygen level-dependent (BOLD) contrast in the breast. *J Magn Reson Imaging*. 2010;32(1):120–129. [PubMed] [Google Scholar]
76. Asghar Butt S, Sogaard LV, Ardenkjaer-Larsen JH, et al. Monitoring mammary tumour progression and effect of tamoxifen treatment in MMTV-PymT using MRI and magnetic resonance spectroscopy with hyperpolarized [1-13C]pyruvate. *Magn Reson Med*. 2015;73(1):51–58. [PubMed] [Google Scholar]
77. Ouwerkerk R, Bleich KB, Gillen JS, Pomper MG, Bottomley PA. Tissue sodium concentration in human brain tumours as measured with 23Na MR imaging. *Radiology*. 2003;227(2):529–537. [PubMed] [Google Scholar]
78. Zaric O, Pinker K, Zbyn S, et al. Quantitative sodium MR imaging at 7 T: initial results and comparison with diffusion-weighted imaging in patients with breast tumours. *Radiology*. 2016;280(1):39–48. [PubMed] [Google Scholar]
79. Klomp DW, van de Bank BL, Raaijmakers A, et al. 31P MRSI and 1H MRS at 7 T: initial results in human breast cancer. *NMR Biomed*. 2011;24(10):1337–1342. [PubMed] [Google Scholar]
80. Wijnen JP, van der Kemp WJ, Luttje MP, Korteweg MA, Luijten PR, Klomp DW. Quantitative (31) P magnetic resonance spectroscopy of the human breast at 7 T. *Magn Reson Med*. 2011. [PubMed] [Google Scholar]

81. Thakur SB BL, Ishill NM, et al. Comparisons of water-to-fat ratios in malignant, benign breast lesions, and normal breast parenchyma: an in vivo proton MRS study. In Proceedings of the 14th Annual Meeting of ISMRM Seattle, Washington, USA 2006: Abstract 2874. [Google Scholar]
82. Thakur SB BL, Ishill NM, et al. Discrimination of choline-positive invasive breast carcinomas using water-to-fat ratio: a proton MRS Study. In Proceedings of the 14th Annual Meeting of ISMRM Seattle, Washington, USA 2006: Abstract 578. [Google Scholar]
83. Freed M, Storey P, Lewin AA, et al. Evaluation of breast lipid composition in patients with benign tissue and cancer by using multiple gradient-echo MR imaging. *Radiology*. 2016;281(1):43–53. [PMC free article] [PubMed] [Google Scholar]
84. Ward KM, Aletras AH, Balaban RS. A new class of contrast agents for MRI based on proton chemical exchange dependent saturation transfer (CEST). *J Magn Reson*. 2000;143(1):79–87. [PubMed] [Google Scholar]
85. Schmitt B, Zamecnik P, Zaiss M, et al. A new contrast in MR mammography by means of chemical exchange saturation transfer (CEST) imaging at 3 Tesla: preliminary results. *Rofo*. 2011; 183(11):1030–1036. [PubMed] [Google Scholar]
86. Schmitt B, Trattng S, Schlemmer HP. CEST-imaging: a new contrast in MR-mammography by means of chemical exchange saturation transfer. *Eur J Radiol*. 2012;81(Suppl. 1):S144–146. [PubMed] [Google Scholar]
87. Desmond KL, Moosvi F, Stanisz GJ. Mapping of amide, amine, and aliphatic peaks in the CEST spectra of murine xenografts at 7 T. *Magn Reson Med*. 2014;71(5):1841–1853. [PubMed] [Google Scholar]
88. deSouza NM, Riches SF, Vanas NJ, et al. Diffusion-weighted magnetic resonance imaging: a potential non-invasive marker of tumour aggressiveness in localized prostate cancer. *Clin Radiol*. 2008;63(7):774–782. [PubMed] [Google Scholar]
89. Brindle KM, Bohndiek SE, Gallagher FA, Kettunen MI. Tumour imaging using hyperpolarized <sup>13</sup>C magnetic resonance spectroscopy. *Magn Reson Med*. 2011. ;66(2):505–519. [PubMed] [Google Scholar]
90. Albers MJ, Bok R, Chen AP, et al. Hyperpolarized <sup>13</sup>C lactate, pyruvate, and alanine: noninvasive biomarkers for prostate cancer detection and grading. *Cancer Res*. 2008;68(20):8607–8615. [PMC free article] [PubMed] [Google Scholar]
91. Tessem MB, Swanson MG, Keshari KR, et al. Evaluation of lactate and alanine as metabolic biomarkers of prostate cancer using <sup>1</sup>H HR-MAS spectroscopy of biopsy tissues. *Magn Reson Med*. 2008;60(3):510–516. [PMC free article] [PubMed] [Google Scholar]
92. Keshari KR, Sai V, Wang ZJ, Vanbrocklin HF, Kurhanewicz J, Wilson DM. Hyperpolarized [<sup>1-13</sup>C]dehydroascorbate MR spectroscopy in a murine model of prostate cancer: comparison with <sup>18</sup>F-FDG PET. *J Nucl Med*. 2013;54(6):922–928. [PMC free article] [PubMed] [Google Scholar]
93. Partridge SC, Ziadloo A, Murthy R, et al. Diffusion tensor MRI: preliminary anisotropy measures and mapping of breast tumours. *J Magn Reson Imaging*. 2010;31 (2):339–347. [PubMed] [Google Scholar]
94. Baltzer PA, Schafer A, Dietzel M, et al. Diffusion tensor magnetic resonance imaging of the breast: a pilot study. *EurRadiol*. 2011;21(1):1–10. [PubMed] [Google Scholar]
95. Bokacheva L, Kaplan JB, Giri DD, et al. Intravoxel incoherent motion diffusion-weighted MRI at 3.0 T differentiates malignant breast lesions from benign lesions and breast parenchyma. *J Magn Reson Imaging*. 2014;40(4):813–823. [PMC free article] [PubMed] [Google Scholar]
96. Kim Y, Ko K, Kim D, et al. Intravoxel incoherent motion diffusion-weighted MR imaging of breast cancer: association with histopathological features and subtypes. *Br J Radiol*. 2016;89(1063):20160140. [PMC free article] [PubMed] [Google Scholar]
97. Cho GY, Moy L, Kim SG, et al. Evaluation of breast cancer using intravoxel incoherent motion (IVIM) histogram analysis: comparison with malignant status, histological subtype, and molecular prognostic factors. *EurRadiol*. 2015. [PMC free article] [PubMed] [Google Scholar]
98. Cho GY GL, Sutton EJ, Zabor EC, et al. Intravoxel incoherent motion (IVIM) histogram biomarkers for prediction of neoadjuvant treatment response in breast cancer patients. *Eur J Radiol Open*. 2017;4:101–107. [PMC free article] [PubMed] [Google Scholar]
99. Nogueira L, Brandao S, Matos E, et al. Application of the diffusion kurtosis model for the study of breast lesions. *EurRadiol*. 2014;24(6): 1197–1203. [PubMed] [Google Scholar]
100. Sun K, Chen X, Chai W, et al. Breast cancer: diffusion kurtosis MR imaging-diagnostic accuracy and correlation with clinical-pathologic factors. *Radiology*. 2015;277(1 ):46–55. [PubMed] [Google Scholar]
101. Alduk AM, Brcic I, Podolski P, Prutki M. Correlation of MRI features and pathohistological prognostic factors in invasive ductal breast carcinoma. *Acta Clin Belg*. 2016:1–7. [PubMed] [Google Scholar]
102. Dietzel M, Baltzer PA, Vag T, et al. Application of breast MRI for prediction of lymph node metastases —systematic approach using 17 individual descriptors and a dedicated decision tree. *Acta Radiol*. 2010;51(8):885–894. [PubMed] [Google Scholar]
103. Kaiser CG, Herold M, Krammer J, et al. Prognostic value of “prepectoral edema” in MR-mammography. *Anticancer Res*. 2017;37(4):1989–1995. [PubMed] [Google Scholar]

104. Wu J, Li B, Sun X, et al. Heterogeneous enhancement patterns of tumour-adjacent parenchyma at MR imaging are associated with dysregulated signaling pathways and poor survival in breast cancer. *Radiology*. 2017;162823. [PMC free article] [PubMed] [Google Scholar]
105. Bae MS, Shin SU, Ryu HS, et al. Pretreatment MR imaging features of triple-negative breast cancer: association with response to neoadjuvant chemotherapy and recurrence-free survival. *Radiology*. 2016;281(2):392–400. [PubMed] [Google Scholar]
106. KizildagYirgin I, Arslan G, Ozturk E, et al. Diffusion weighted MR imaging of breast and correlation of prognostic factors in breast cancer. *Balkan Med J*. 2016;33(3):301–307. [PMC free article] [PubMed] [Google Scholar]
107. Durando M, Gennaro L, Cho GY, et al. Quantitative apparent diffusion coefficient measurement obtained by 3.0Tesla MRI as a potential noninvasive marker of tumour aggressiveness in breast cancer. *Eur J Radiol*. 2016;85(9):1651–1658. [PMC free article] [PubMed] [Google Scholar]
108. Rabasco P, Caivano R, Simeon V, et al. Can diffusion-weighted imaging and related apparent diffusion coefficient be a prognostic value in women with breast cancer? *Cancer Invest*. 2017;35(2):92–99. [PubMed] [Google Scholar]
109. Cancer Genome Atlas N. Comprehensive molecular portraits of human breast tumours. *Nature*. 2012;490(7418):61–70. [PMC free article] [PubMed] [Google Scholar]
110. Sorlie T, Perou CM, Tibshirani R, et al. Gene expression patterns of breast carcinomas distinguish tumour subclasses with clinical implications. *Proc Natl Acad Sci U S A*. 2001. ;98(19): 10869–10874. [PMC free article] [PubMed] [Google Scholar]
111. Goldhirsch A, Winer EP, Coates AS, et al. Personalizing the treatment of women with early breast cancer: highlights of the St Gallen International Expert Consensus on the Primary Therapy of Early Breast Cancer 2013. *Ann Oncol*. 2013;24(9):2206–2223. [PMC free article] [PubMed] [Google Scholar]
112. Mazurowski MA, Zhang J, Grimm LJ, Yoon SC, Silber JI. Radiogenomic analysis of breast cancer: luminal B molecular subtype is associated with enhancement dynamics at MR imaging. *Radiology*. 2014;273(2):365–372. [PubMed] [Google Scholar]
113. Shin HJ, Kim HH, Huh MO, et al. Correlation between mammographic and sonographic findings and prognostic factors in patients with node-negative invasive breast cancer. *Br J Radiol*. 2011;84(997):19–30. [PMC free article] [PubMed] [Google Scholar]
114. Elias SG, Adams A, Wisner DJ, et al. Imaging features of HER2 overexpression in breast cancer: a systematic review and meta-analysis. *Cancer Epidemiol Biomarkers Prev*. 2014;23(8):1464–1483. [PubMed] [Google Scholar]
115. Grimm LJ, Johnson KS, Marcom PK, Baker JA, Soo MS. Can breast cancer molecular subtype help to select patients for preoperative MR imaging? *Radiology*. 2015;274(2):352–358. [PubMed] [Google Scholar]
116. Kim EJ, Kim SH, Park GE, et al. Histogram analysis of apparent diffusion coefficient at 3.0T: Correlation with prognostic factors and subtypes of invasive ductal carcinoma. *J Magn Reson Imaging*. 2015;42(6):1666–1678. [PubMed] [Google Scholar]
117. Uematsu T MR imaging of triple-negative breast cancer. *Breast Cancer*. 2011; 18(3):161–164. [PubMed] [Google Scholar]
118. Waugh SA, Purdie CA, Jordan LB, et al. Magnetic resonance imaging texture analysis classification of primary breast cancer. *EurRadiol*. 2016;26(2):322–330. [PubMed] [Google Scholar]
119. Grimm LJ, Zhang J, Mazurowski MA. Computational approach to radiogenomics of breast cancer: luminal A and luminal B molecular subtypes are associated with imaging features on routine breast MRI extracted using computer vision algorithms. *J Magn Reson Imaging*. 2015;42(4):902–907. [PubMed] [Google Scholar]
120. Li H, Zhu Y, Burnside ES, et al. MR imaging radiomics signatures for predicting the risk of breast cancer recurrence as given by research versions of MammaPrint, Oncotype DX, and PAM50 gene assays. *Radiology*. 2016;281(2):382–391. [PMC free article] [PubMed] [Google Scholar]
121. Sutton EJ, Dashevsky BZ, Oh JH, et al. Breast cancer molecular subtype classifier that incorporates MRI features. *J Magn Reson Imaging*. 2016;44(1):122–129. [PMC free article] [PubMed] [Google Scholar]
122. Ashraf AB, Daye D, Gavenonis S, et al. Identification of intrinsic imaging phenotypes for breast cancer tumours: preliminary associations with gene expression profiles. *Radiology*. 2014;272(2):374–384. [PMC free article] [PubMed] [Google Scholar]